LRP 702/01 July 2001

Effect of ELMs on the Measurement of Vertical Plasma Position in TCV and JET

F. Hofmann, I. Furno, S. Gerasimov, Y. Martin,
F. Milani, M.F.F. Nave, H. Reimerdes,
F. Sartori, O. Sauter

Accepted for publication in
Nuclear Fusion

ISSN 0458-5895

Effect of ELMs on the Measurement of Vertical Plasma Position in TCV and JET

F. Hofmann[1], I. Furno[1], S. Gerasimov[2], Y. Martin[1], F. Milani[2], M.F.F. Nave[3], H. Reimerdes[1], F. Sartori[2], O. Sauter[1]

[1]*Centre de Recherches en Physique des Plasmas, Association EURATOM - Confédération Suisse, Ecole Polytechnique Fédérale de Lausanne, CH-1015 Lausanne, Switzerland*

[2]*UKAEA, Culham Science Centre, Abingdon, Oxfordshire OX14 3DB, United Kingdom*

[3]*Associação EURATOM/IST, Inst. Superior Tecnico, 1049-001 Lisbon, Portugal*

Abstract

The effect of ELMs on the vertical position observer in TCV has been investigated and a new, optimized observer which minimizes the influence of ELMs has been constructed. The new observer has been tested in TCV, under closed loop conditions, and we have shown that it is considerably less sensitive to ELMs than the classical observer. In order to determine whether this method could also be used in JET, we have analyzed ELMy H-mode pulses and VDEs in JET and we have constructed a modified vertical position observer, optimized for JET conditions. We show that, if this new observer were used in JET, the perturbations caused by ELMs would be greatly reduced.

1. Introduction

Tokamak plasmas with elongated cross-section give access to higher beta values and better confinement than circular plasmas, but they are inherently unstable with respect to an axisymmetric mode, the so-called vertical instability [1]. This mode must be stabilized by a combination of a passive shell and active feedback coils. One of the key elements of the feedback system in an elongated tokamak is the vertical position observer, i.e. the measurement of the vertical plasma position and/or velocity in real time. The classical method of measuring the vertical plasma position in a tokamak, i.e. the current moment method [2], is sometimes difficult to implement because the ideal measuring contour may be inaccessible. In practice, the measurement is usually obtained from a linear combination of magnetic field probe and flux loop signals and, consequently, it can be perturbed by plasma effects, such as sawteeth, ELMs and non-axisymmetric MHD modes, which are not necessarily related to the vertical displacement instability. Some of these perturbations, e.g. n>0 modes, can be eliminated by a judicious combination of magnetic probe arrays, located at different toroidal positions, but other effects, such as ELMs, will always have an influence on the vertical position control system [3]. ELMs produce two distinct effects in an elongated tokamak: On the one hand, they give rise to short-lived magnetic perturbations, inducing eddy currents in passive structures, which can affect the vertical position measurement. On the other hand, they produce a drop in plasma stored energy and a modification of the current profile, which causes the equilibrium to change significantly. In up-down asymmetric configurations, such as single-null divertors, the second effect implies a rapid vertical displacement of the plasma current centroid. In the case of small or medium size ELMs, the two effects occur simultaneously and are difficult to separate. In the case of very large or giant ELMs, the second effect is dominant [4]. In this paper, we do not consider giant ELMs.

A method to mitigate the influence of ELMs on the vertical position control system consists of switching off the vertical feedback for a short time interval during each ELM. This method obviously requires a reliable ELM detector for triggering the feedback cut and it can only be used if the growth time of the vertical instability is much longer than the duration of a typical ELM. The method has been used in JET, but has not given convincing evidence of a real benefit. In this paper, we propose a different method for reducing ELM perturbations. First, we investigate the effect of ELMs on the vertical position observer in TCV and we show that a modification of the classical observer can greatly reduce its sensitivity to ELMs. Then, we analyze ELMy H-mode pulses and VDEs in JET and, using the same procedure as was used in TCV, we construct a new vertical position observer for JET with reduced ELM sensitivity.

2. ELMy H-mode in TCV

Steady-state ELMy H-mode plamas are produced routinely in TCV [5-9]. Recently, it has been shown that, in order to access the ELMy H-mode under Ohmic conditions in TCV, both the plasma density and the current must be chosen within narrow windows [9]. Once the L-H transition has taken place, density and current can be varied in fairly wide ranges without loosing the ELMy H-mode. Here, we consider an Ohmic, single-null divertor discharge, whose ion grad B drift is in the unfavourable direction, i.e. away from the X-point (Fig.1). This plasma is characterized by a relatively high elongation (κ=2) and, consequently, a high growth rate of the vertical instability (γ=1300 s^{-1}). The ELM frequency is 170 Hz (Fig.2) and the average energy loss per ELM is approximately 3%. The question whether these ELMs are Type I or Type III cannot be answered unambiguously since we are dealing with Ohmic H-modes and the heating power cannot be changed without changing other important plasma

parameters. However, the fact that the ELMs appear after a short ELM-free period indicates that they are more likely to be Type I than Type III.

3. The TCV vertical position control system

TCV has a unique vertical position control system using active feedback coils both outside and inside the vacuum vessel [10]. The external coils (F-coils in Fig.1) are driven by slow power supplies with a response time of ~1 ms. They are used for proportional and derivative feedback. The internal coils (G-coils) are driven by a fast supply with a response time of less that 0.1ms and are used for derivative feedback only. The system allows the stabilization of elongated plasmas with very high growth rates and extremely low stability margins [10].

The fast loop uses a vertical position observer consisting of a linear combination of magnetic field probe signals. The probes are installed inside the vacuum vessel in several poloidal planes [11]. For vertical position control, we use average signals of two poloidal arrays which are displaced toroidally by 180^0. The probes measure the poloidal field parallel to the vessel wall. They are distributed uniformly over the poloidal circumference and they are numbered clockwise, from 1 to 38, starting from the inboard midplane. The coefficients which are used to construct the vertical position signal are shown in Fig.3a. They are assumed to be proportional to the perturbed magnetic field at the probe positions, produced by a small vertical displacement of the plasma. Note that probes 13-16 and 24-27 are not used in this observer, i.e. their coefficients are zero. This choice is motivated by the fact that these probes are located in the vicinity of the internal active coils (G1, G2) and that we wish to avoid direct coupling between the active coils and the observer. It should be noted that the observer (Fig. 3a) is not up-down symmetric. This is a consequence of the fact that the plasma is located in the upper half of the vessel (Fig.1) and that the observer is designed to give zero output when the plasma

vertical position corresponds to its reference value [12].

4. Perturbation of the poloidal magnetic field by ELMs in TCV

Fig.4 shows a contour plot of the perturbed poloidal magnetic field, produced by a typical ELM, as a function of time and position on the poloidal circumference. At time t=0.6445s, we see the ELM structure and immediately afterwards, a damped oscillation appears (probe numbers 14 and 26), which is due to an oscillating current in the G-coils. This oscillation is triggered by the ELM through the vertical position control loop.

Figure 3b shows the poloidal field perturbation produced by a typical ELM as a function of probe number. Here, we plot the poloidal field difference between the time when the ELM perturbation reaches its maximum and the time immediately preceeding the ELM. The measurement was performed under closed loop conditions. As a result, we see both the signature of the ELM and the effect of the current pulse in the internal active coil (peaks at #14 and #26). The ELM signature can be compared with a typical VDE signature. Figure 3c shows poloidal field measurements during a VDE which was induced by a feedback cut. We note that VDE and ELM signatures are quite different and this difference allows us to construct an ELM-resistant observer. We also note that the observer and the VDE signature are similar, but not identical. This is due to the fact that the observer was constructed by assuming a rigid vertical displacement of the entire plasma, whereas the VDE is subject to plasma deformation and thus consists of a superposition of many poloidal harmonics [13].

5. Construction and test of an ELM-resistant vertical position observer

Using the measurements presented above, we can now proceed to the construction of a new observer which satisfies the following four constraints: (1) the new observer coefficients

must be orthogonal to the fast ELM response, (2) the new observer must give the same response to a rigid vertical displacement of the plasma (or a VDE) as did the old observer, (3) the coefficients 13-16 and 24-27 must be zero to avoid coupling with the active coil and (4) the difference between the new and old observer coefficients should be minimized in the least squares sense. This last condition is introduced to obtain a unique solution and to exclude solutions with only one or two non-zero coefficients. The optimization procedure, as outlined above, can be written as

$$S = (\boldsymbol{N} - \boldsymbol{C})^2 + \lambda_1(\boldsymbol{N} \cdot \boldsymbol{E}) + \lambda_2((\boldsymbol{N} \cdot \boldsymbol{V}) - (\boldsymbol{C} \cdot \boldsymbol{V}))$$

$$\frac{\partial S}{\partial N_i} = 0, \frac{\partial S}{\partial \lambda_i} = 0$$

where the vectors N, C, E and V contain the coefficients of the new observer, the old obsrever, the ELM response and the VDE response, respectively.

The result (Fig. 5) shows that a minor modification of the observer coefficients is sufficient for satisfying the constraints mentioned above. It is important to note that, since both the ELM response and the VDE response depend on plasma parameters (shape, current distribution, etc.), the new observer will also depend on these parameters. In TCV, this poses no particular problem since the observer coefficients are always computed specifically for each discharge [12].

The new observer was tested in TCV by applying it to a typical steady-state ELMy H-mode plasma (Fig.2). ELM effects of the old and new observers are compared in Fig.6. It is seen that the new observer reduces the voltage pulses in the fast control loop by at least a factor of 5 (Figs. 6b and 6e). The vertical plasma position, as obtained from off-line equlibrium

reconstructions, is shown in Figs. 6c and 6f. We note that the position excursion produced by each ELM is much smaller in the case of the new observer (Fig. 6f) than it is with the old observer (Fig. 6c). From these results we conclude that the perturbations produced by ELMs in the TCV vertical position control system can be significantly reduced by using an optimized vertical position observer. A contour plot of the perturbed poloidal magnetic field in the case when the new observer is used (Fig.7) shows that although the ELM structure is the same as with the old observer, the damped oscillation has disappeared almost completely.

The improved performance of the new observer can also be seen in soft X-ray measurements. In Figure 8, we present the D-alpha signal from the edge of the plasma (top row), the soft X-ray emission from the centre of the plasma (second row), the vertical plasma position as obtained from soft X-ray tomography (third row) and, for comparison, the vertical plasma position obtained form off-line equlibrium reconstructions (bottom row). The discharge shown in this Figure is characterized by a switch of observers in real time. Before t=0.5 s, the old observer was active, whereas after 0.5 s, the new observer was switched on. The Figure shows that the sawtooth crashes produce large perturbations in the vertical position measurement as obtained from soft X-ray tomography. This is to be expected since the soft X-ray measurement predominantly sees the central region of the plasma. However, the sawteeth have no influence on the magnetic vertical position observer, which was actually used in the feedback loop. This is evident from the bottom frames in Fig. 8, showing the Z-position obtained from off-line equilibrium reconstructions. Figure 8 also shows that the vertical position excursion produced by ELMs is much smaller with the new observer than it is with the old one, which confirms the magnetic measurements presented in Fig.6.

An obvious question is whether the new observer has any disadvantages with respect to the old one. We have made an attempt to answer this question by computing the sensitivity of

the two observers to non-axisymmetric MHD modes such as those which are commonly seen in TCV. We assume a rotating, resonant current perturbation with mode structure m/n=3/2, located on the q=1.5 surface. The amplitude of the perturbation corresponds to a large island, with a width of 35mm, which is consistent with measurements of MHD modes in TCV. We then compute the observer output signals produced by this mode, and we find that the sensitivity of the new observer is 25% higher than that of the old observer. However, these output signals should be compared to the output resulting from a small vertical displacement. The result of this comparison is that, with the old observer, a typical m/n=3/2 mode produces an output which is equivalent to a vertical displacement of 0.9mm, whereas with the new observer, the output is equivalent to a displacement of 1.1mm. In this context, it should be noted that the vertical position control system in TCV is designed to cope with sudden vertical displacements of the order of 10mm. In addition, MHD modes with n>1 have typical rotation frequencies of 10kHz or higher and, at these frequencies, the signal attenuation in the vertical position control loop is more than an order of magnitude. We conclude that, while the new observer has a slightly higher sensitivity to m/n=3/2 modes than the old one, the observer output signals resulting from these modes are small compared to the output produced by typical vertical displacements.

6. An ELM-resistent observer for JET

In JET, operation at high elongation has often been limited by the performance of the vertical position control system and, in particular, by the perturbing effects of ELMs [4, 14]. Two distinct problems have been encountered. The first occurs in pulses with high ELM frequency and long duration. Each ELM translates into a series of spurious switchings of the Fast Radial Field Amplifier and this can cause overheating and eventually trip the amplifier. The

second problem is caused by giant ELMs which often occur after a long ELM-free phase. Here, the instantaneous energy loss and the resulting rapid vertical displacement of the plasma are so large that the amplifier current saturates and vertical position control is lost [14].

The vertical velocity observer in JET [15, 16] uses non-integrated signals from 9 magnetic field probes, located inside the vacuum vessel, in the upper half-plane of the poloidal cross-section and 14 saddle loops, located outside the vessel as shown in Fig. 9. The probes in the lower half-plane are not used because they are partially shielded from the plasma by the divertor structure. Assuming that the fast response of the vertical velocity observer is dominated by the magnetic probe signals, we can measure ELM and VDE signatures in JET, using the same method as was used in TCV (section 4). Figure 10a shows the ELM response in JET as obtained from averaging over four large ELMs. The ELM frequency in this pulse is 16 Hz, the ELMs are Type I, and the average energy loss per ELM is approximately 6%. Figure 10b shows the signature of a VDE which was produced intentionally by switching off the vertical feedback. The vertical velocity observer presently used in the JET and a new observer, which was obtained by applying the optmization procedure outlined in section 5, are shown in Fig. 10c. We note that, in the case of JET, the new observer is radically different from the old one. In order to assess the quality of the new observer, we compute new and old observer outputs during a typical VDE (JET pulse 50691) and during an ELMy H-mode (JET pulse 50810). The results (Fig. 11) show that, while the VDE outputs of the two observers are identical, the ELM perturbation is reduced by more than a factor of two in the case of the new observer.

7. Conclusions

In TCV, the effect of ELMs on the poloidal magnetic field has been measured and an ELM-resistent vertical position observer has been constructed which differs but little from the

classical observer. The new observer has been tested and it is shown that it reduces the perturbations due to ELMs by a large factor. In JET, an analysis of recent ELMy H-mode pulses shows that a similar optimization of the vertical position observer is possible. An ELM-resistent observer has been developed for JET and it is shown that, if it were implemented, it would reduce the ELM perturbations by a factor of two. We expect that even better results could be obtained, in the case of JET, if it were possible to install and to use additional magnetic field probes, located close to the plasma boundary, below the equatorial plane of the machine.

Acknowledgements

Fruitful discussions with Dr. Morten Lennholm are gratefully acknowledged. This work has partly been performed under the European Fusion Development Agreement and was partly supported by the Fonds National Suisse de la Recherche Scientifique.

References

[1] Bortnikov, A.V. et al., in Proc. 8th Eur. Conf. Controlled Fusion and Plasma Physics (Prague 1977) Vol I, IAEA, Vienna (1977) 41.

[2] Zakharov, L.E., Shafranov, V.D., Sov. Phys. Tech. Phys. **13** (1973) 151.

[3] Todd, T.N. et al., Plasma Phys. Control. Fusion **35** (1993) B231.

[4] Ali-Arshad, S. et al., in Controlled Fusion and Plasma Physics (Proc. 23rd Eur. Conf. Kiev, 1996), Vol. 20C, Part I, European Physical Society, Geneva (1996) 179.

[5] Hofmann. F. et al., Plasma Phys. Control. Fusion **36** (1994) B277.

[6] Dutch, M.J. et al., Nucl. Fusion **35** (1995) 650.

[7] Duval, B.P. et al., in Controlled Fusion and Plasma Physics (Proc. 22nd Eur. Conf. Bournemouth, 1995), Vol. 19C, Part II, European Physical Society, Geneva (1995)

II-097.

[8] Weisen, H. et al., Plasma Phys. Control. Fusion **38** (1996) 1137.

[9] Martin, Y. et al., in Controlled Fusion and Plasma Physics (Proc. 27th Eur. Conf. Budapest, 2000).

[10] Hofmann, F. et al., Nucl. Fusion **38** (1998) 399.

[11] Moret, J.-M. et al., Rev. Sci. Instrum. **69** (1998) 2333.

[12] Hofmann, F. et al., in Controlled Fusion and Plasma Physics (Proc. 22nd Eur. Conf. Bournemouth, 1995), Vol. 19C, Part II, European Physical Society, Geneva (1995) II-101.

[13] Ward, D.J. et al., Nucl. Fusion **34** (1994) 401.

[14] JET TEAM (presented by A. Tanga) in Fusion Energy 1996 (proc 16th Int. Conf. Montreal 1996) Vol. 1, IAEA, Vienna (1997) 723.

[15] Lennholm, M. et al., Proc. 17th IEEE/NPSS Symposium on Fusion Engineering, San Diego 1997, p. 539.

[16] Lennholm, M. et al., Fusion Engineering and Design **48** (2000) 37..

Figure Captions

Fig.1: ELMy H-mode plasma in TCV: Shot # 18416 at 0.570s, I_P=513kA, B_T=1.45T, κ=2.03, δ=0.45, ELM frequency=170Hz. Feedback for vertical position control is applied to coils F3, F4, F7, F8, G1, G2.

Fig.2: ELMy H-mode discharge in TCV, showing (from top to bottom) D-alpha emission, plasma current, elongation, line averaged electron density and electron temperature on axis.

Fig.3: (a) Coefficients used in the classical vertical position observer in TCV vs. probe number. (b) ELM response (Shot # 18329 at 0.76s), including effect of internal active coils (peaks at probe numbers 14 and 26). (c) Response of a VDE in TCV (Shot # 15971 at 0.605s). The VDE was intentionally produced by a preprogrammed feedback cut.

Fig.4: Perturbed poloidal magnetic field produced by an ELM in TCV, using the classical vertical position observer. The ELM structure, at t=0.6445s, and the effect of oscillating currents in the G-coils are clearly seen.

Fig.5: Comparison of old and new observer coefficients vs. probe number, in TCV.

Fig.6: (a) and (d): D-alpha signals of two identical ELMy H-mode discharges in TCV, (b) and (e): G-coil voltage, proportional to vertical plasma velocity, as obtained from old and new observers, (c) and (f): Vertical plasma displacement, as obtained from LIUQE equilibrium reconstructions at 10 kHz sampling rate.

Fig.7: Perturbed poloidal magnetic field produced by an ELM in TCV, using the optimized vertical position observer. The colour coding of B is identical to that of Fig. 4. Oscillating currents in the G-coils have virtually disappeared.

Fig.8: Comparison of old and new observers in TCV, as seen by soft X-ray measurements in an ELMy H-mode discharge. (a), (b): D-alpha signal. (c), (d): soft X-ray emission from the centre of the plasma. (e), (f): Vertical plasma position as obtained from soft X-ray tomography.

(g), (h): Vertical plasma position obtained from LIUQE equilibrium reconstructions at 10 kHz sampling rate.

Fig.9: Perspective view of magnetic measurements in JET which are used for vertical position control.

Fig.10: (a) ELM response in JET (average of 4 ELMs) as seen by the poloidal magnetic field probes 1 to 9, located in the upper half of the poloidal cross-section. (b) VDE response in JET. (c) Standard (solid line) and optimized (open squares) observer coefficients in JET.

Fig.11: (a) Standard (solid line) and optimized (open squares) observer outputs for a typical VDE in JET. (b) Standard and (c) optimized observer outputs during an ELMy H-mode in JET.

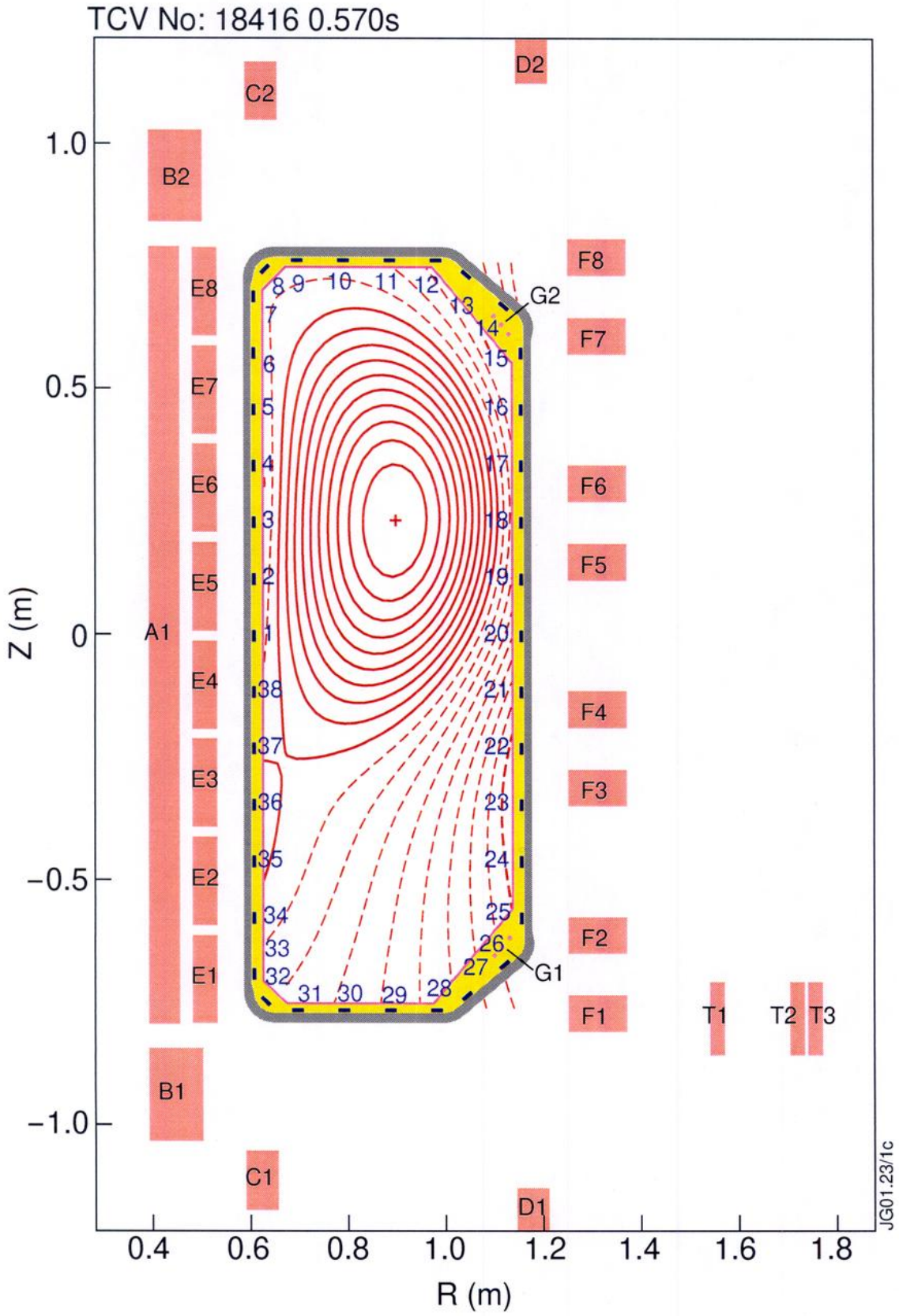
TCV No: 18416 0.570s
D2
C2
B2
F8
G2
F7
E8
E7
E6
F6
E5
F5
A1
E4
F4
E3
F3
E2
F2
G1
E1
F1
T1
T2
T3
B1
C1
D1
Z (m)
R (m)
1.0
0.5
0
−0.5
−1.0
0.4
0.6
0.8
1.0
1.2
1.4
1.6
1.8
JG01.23/1c

Fig. 1

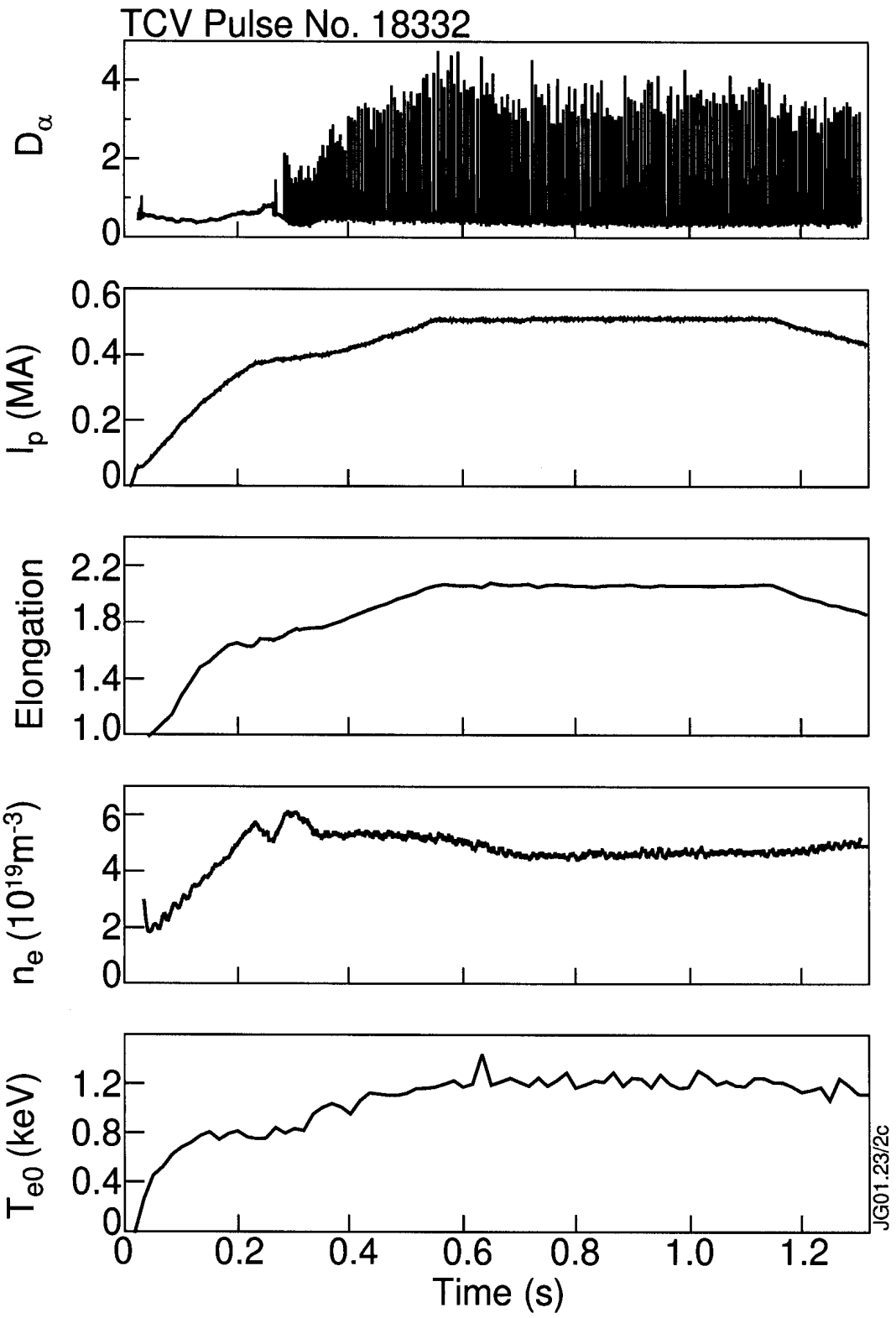
TCV Pulse No. 18332
D_α
4
2
0
I_p (MA)
0.6
0.4
0.2
0
Elongation
2.2
1.8
1.4
1.0
n_e ($10^{19}m^{-3}$)
6
4
2
0
T_{e0} (keV)
1.2
0.8
0.4
0
0
0.2
0.4
0.6
0.8
1.0
1.2
Time (s)
JG01.23/2c

Fig. 2

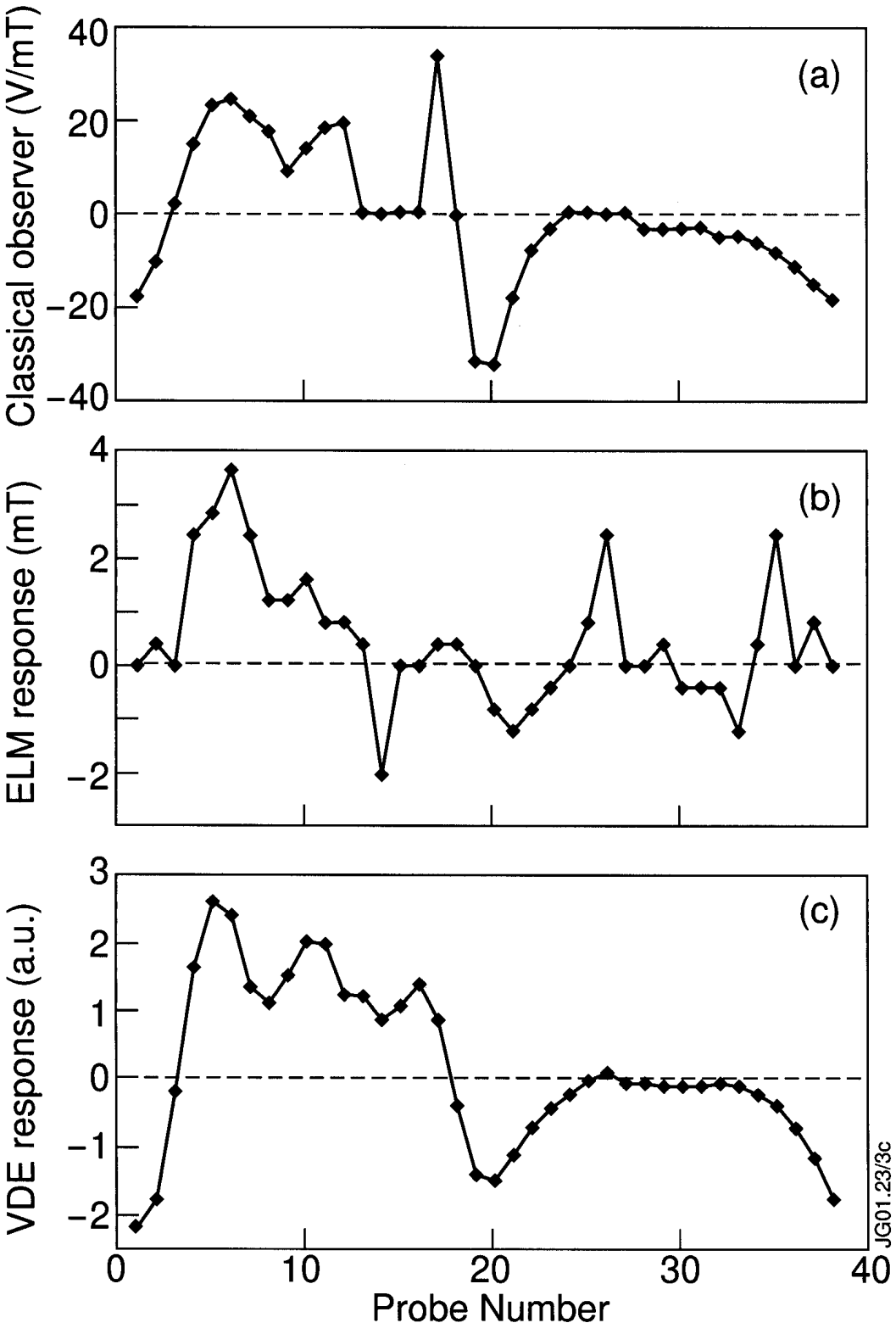
Classical observer (V/mT)
40
20
0
−20
−40
(a)
ELM response (mT)
4
2
0
−2
(b)
VDE response (a.u.)
3
2
1
0
−1
−2
(c)
0
10
20
30
40
Probe Number
JG01.23/3c

Fig. 3

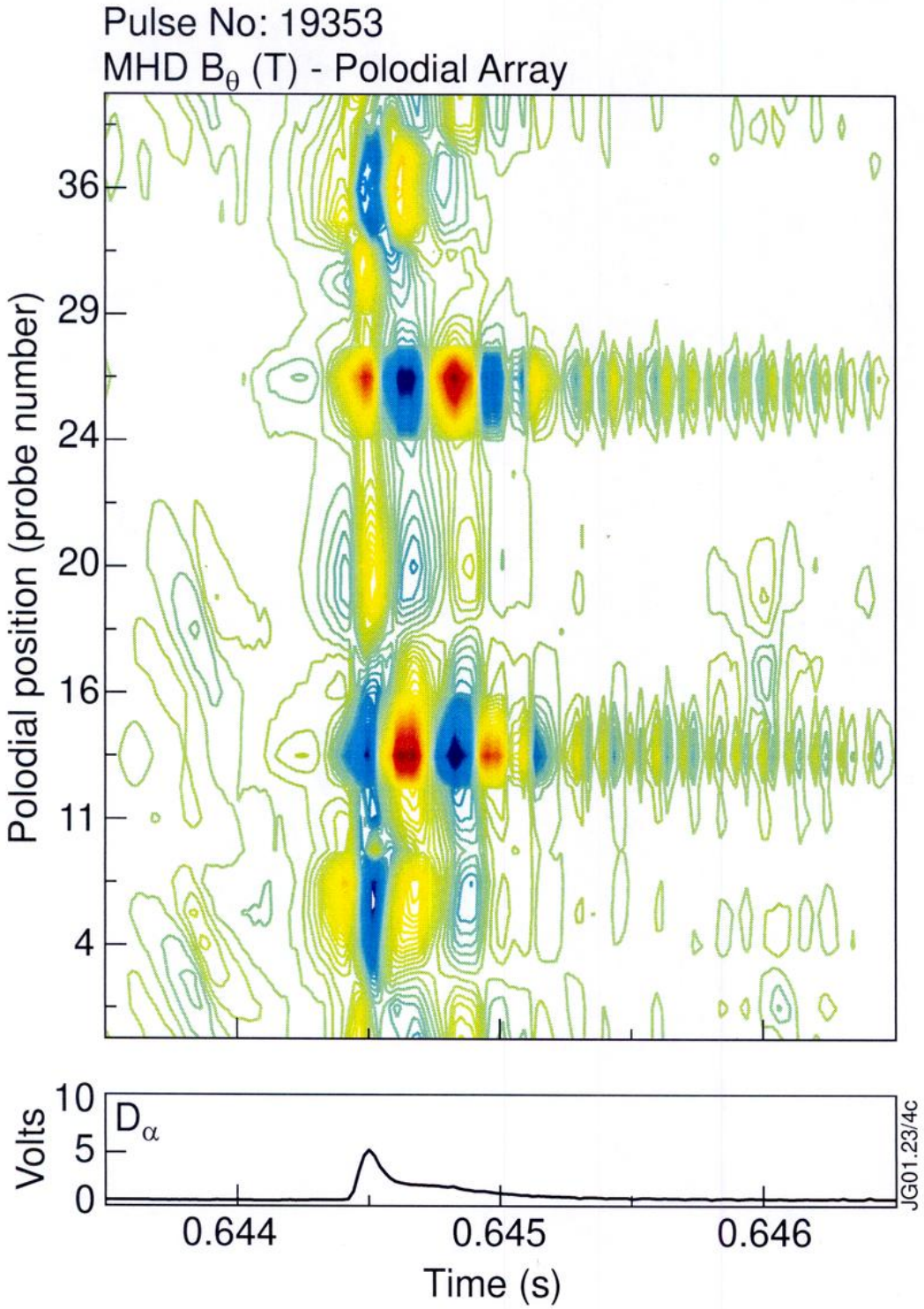
Pulse No: 19353
MHD B_θ (T) - Polodial Array
Polodial position (probe number)
36
29
24
20
16
11
4
Volts
10
5
0
D_α
0.644
0.645
0.646
Time (s)
JG01.23/4c

Fig. 4

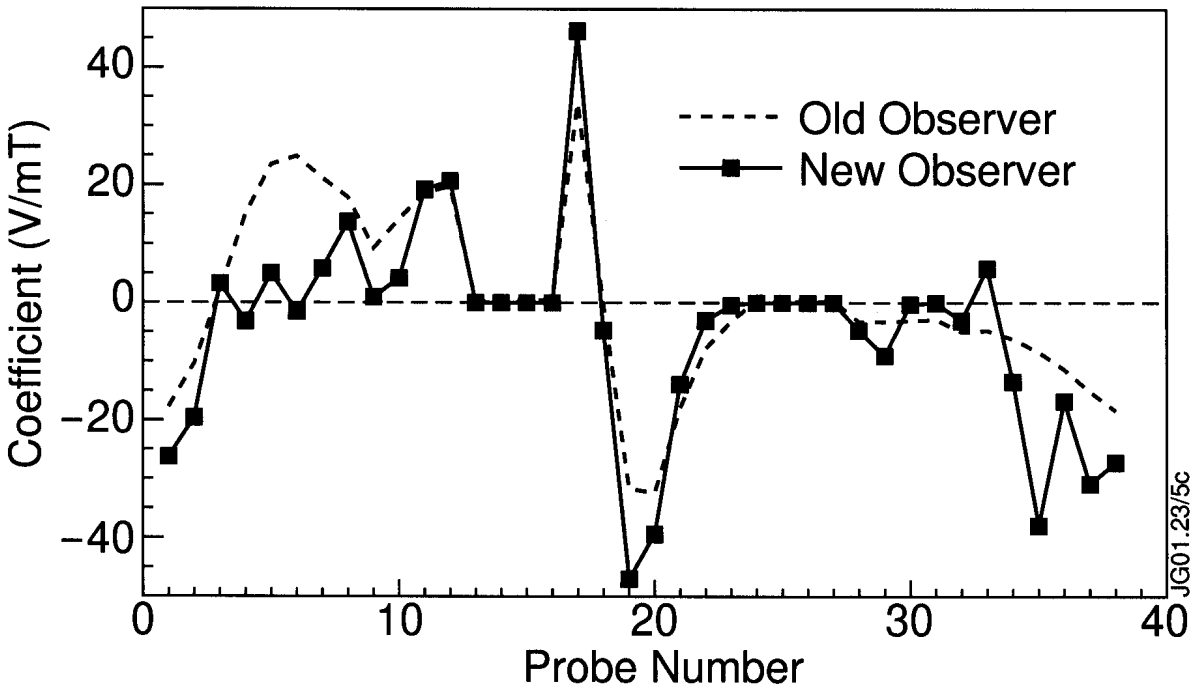
Old Observer
New Observer
Coefficient (V/mT)
Probe Number
40
20
0
−20
−40
0
10
20
30
40
JG01.23/5c

Fig. 5

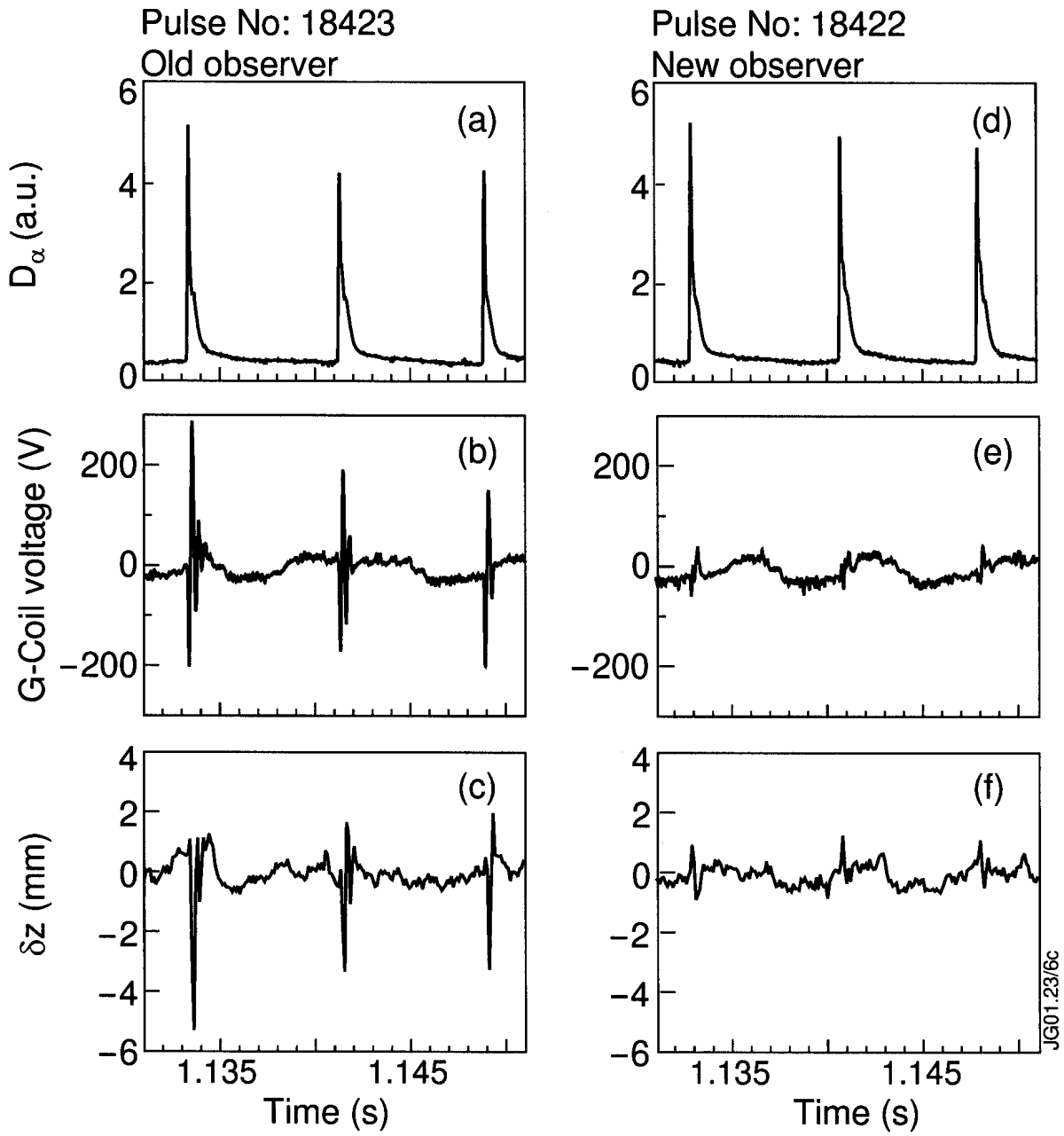
Pulse No: 18423
Old observer
Pulse No: 18422
New observer
D_α (a.u.)
G-Coil voltage (V)
δz (mm)
(a)
(b)
(c)
(d)
(e)
(f)
6
4
2
0
200
0
−200
4
2
0
−2
−4
−6
1.135
1.145
Time (s)
JG01.23/6c

Fig. 6

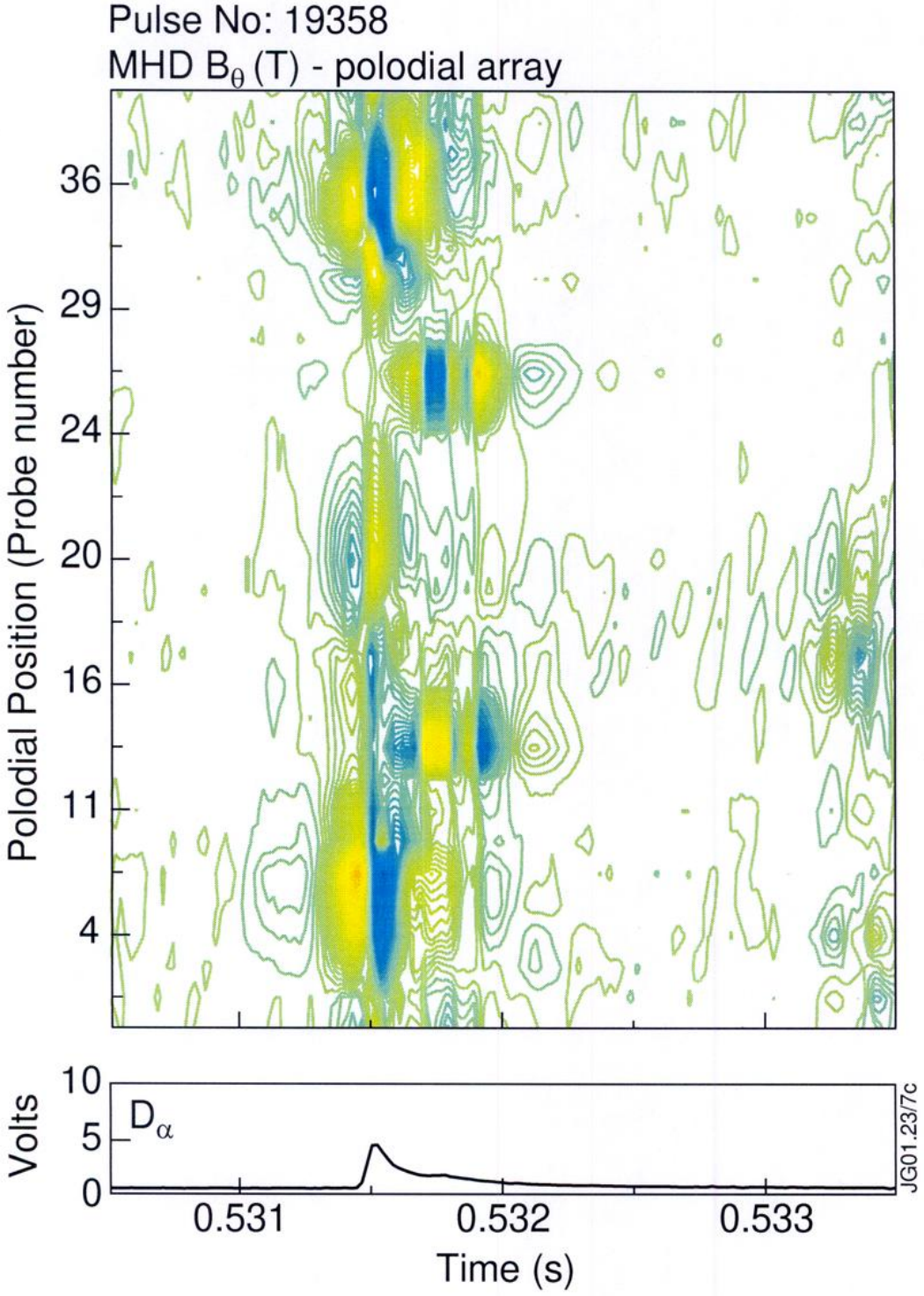
Pulse No: 19358
MHD B_θ (T) - polodial array
Polodial Position (Probe number)
36
29
24
20
16
11
4
Volts
10
5
0
D_α
0.531
0.532
0.533
Time (s)
JG01.23/7c

Fig. 7

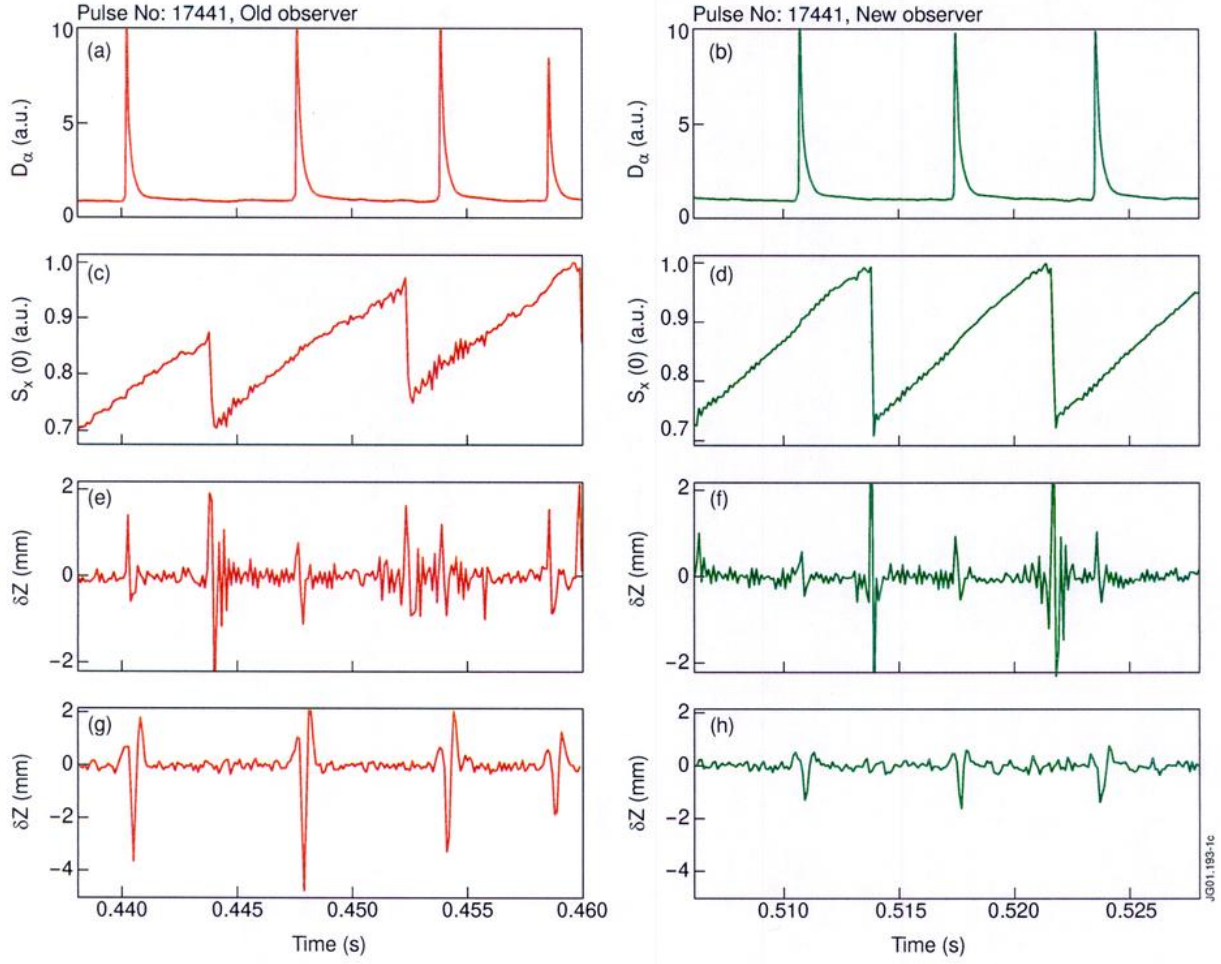
Pulse No: 17441, Old observer
Pulse No: 17441, New observer
(a)
(b)
(c)
(d)
(e)
(f)
(g)
(h)
D_α (a.u.)
S_x (0) (a.u.)
δZ (mm)
Time (s)
JG01.193-1c

Fig. 8

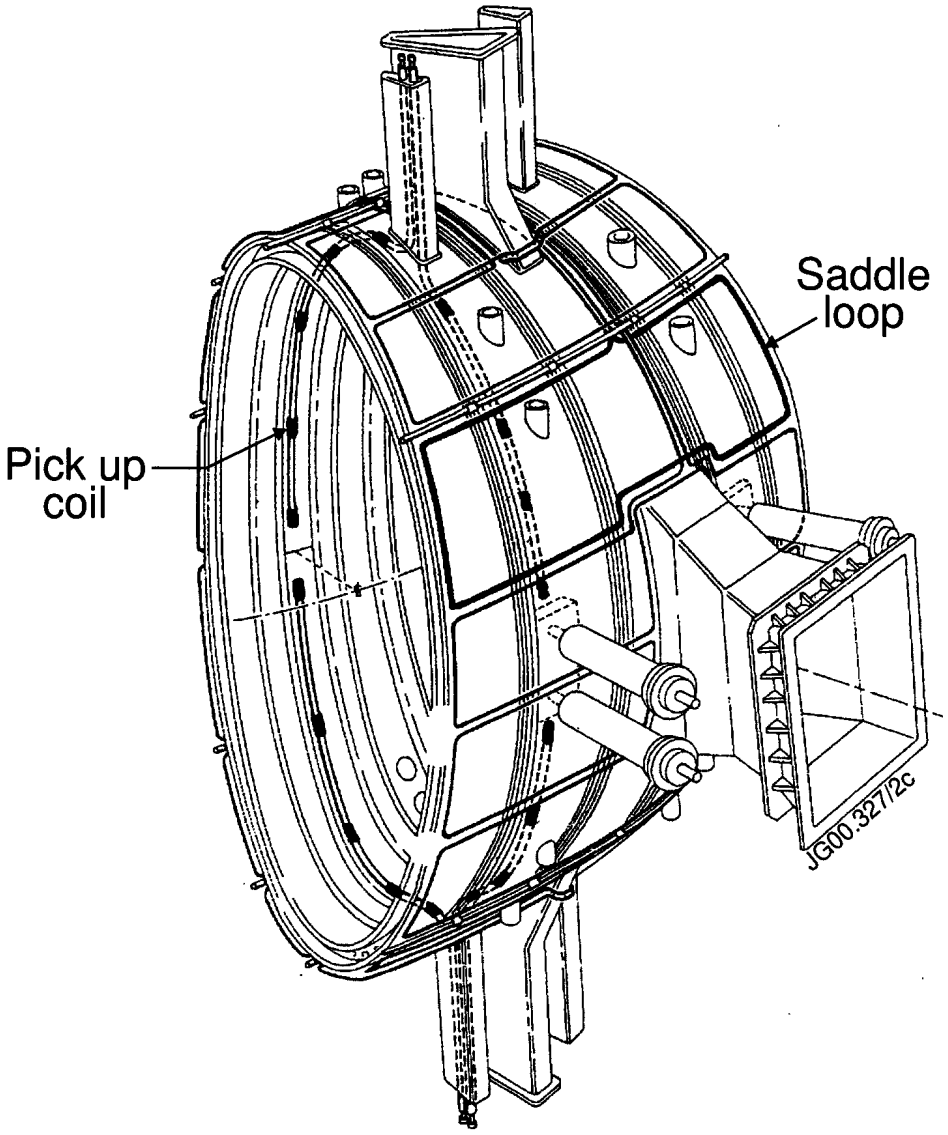

Fig. 9

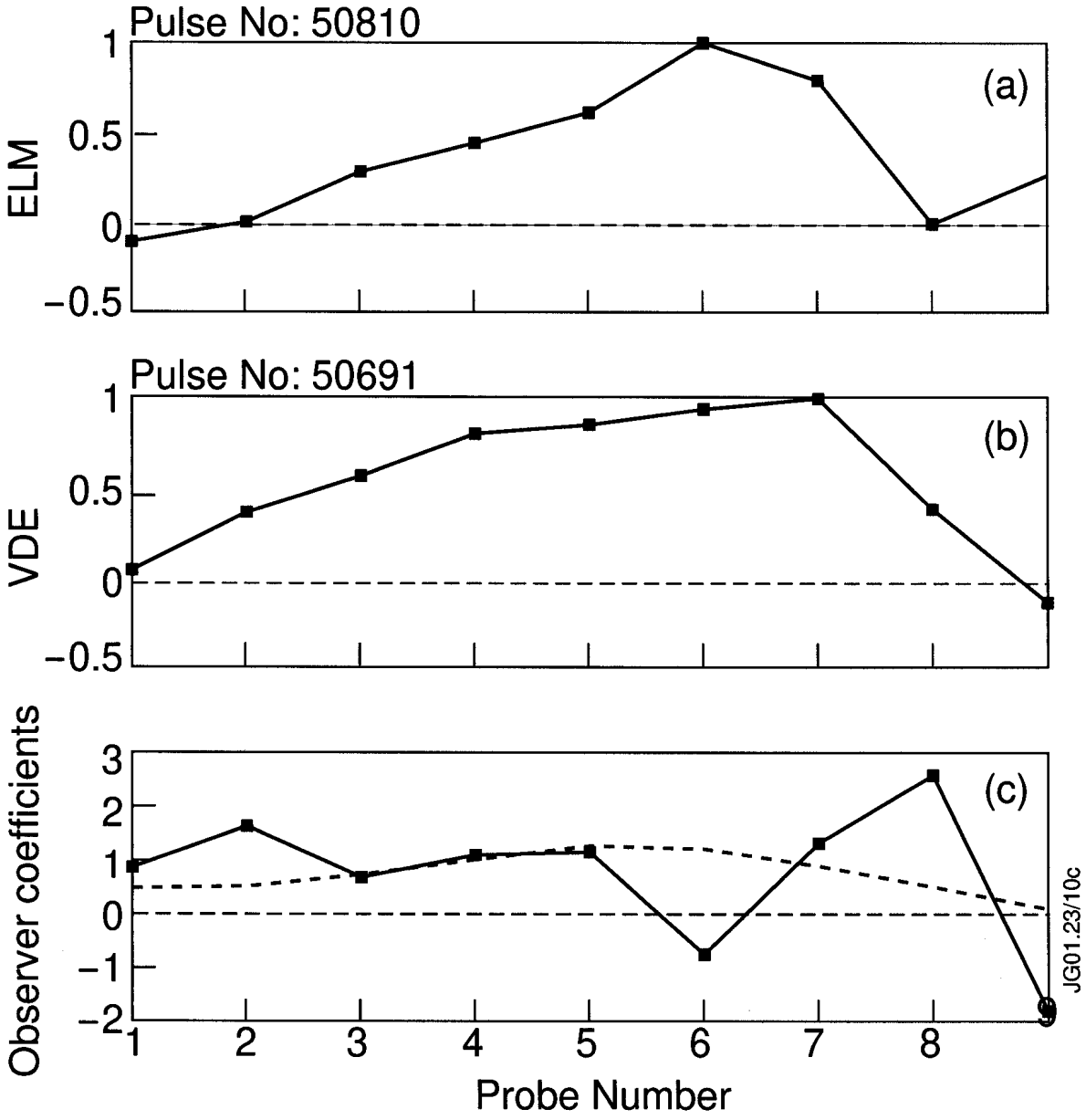
Pulse No: 50810
ELM
(a)
Pulse No: 50691
VDE
(b)
Observer coefficients
(c)
Probe Number
JG01.23/10c

Fig. 10

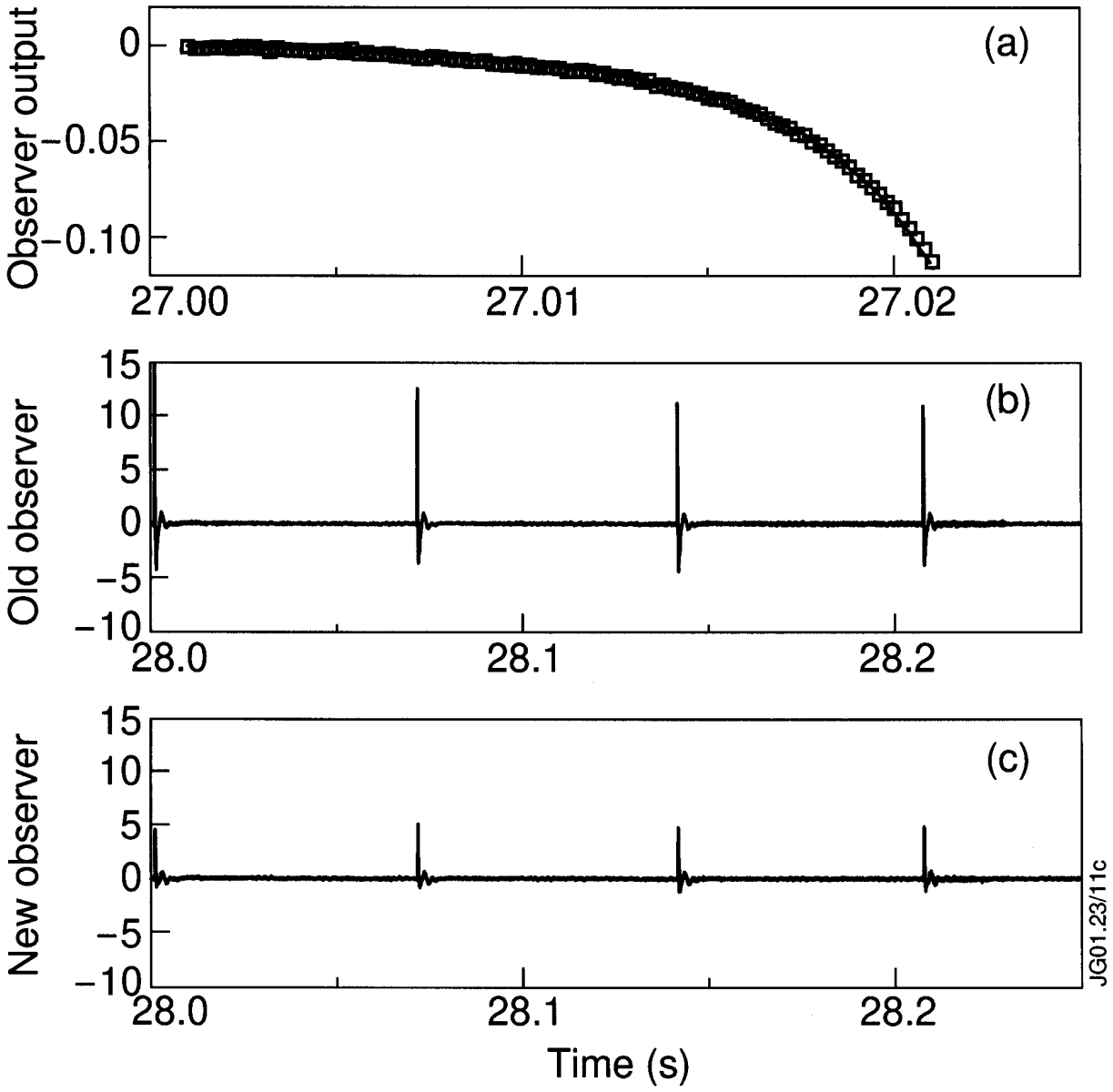
Observer output
0
−0.05
−0.10
27.00
27.01
27.02
(a)
Old observer
15
10
5
0
−5
−10
28.0
28.1
28.2
(b)
New observer
15
10
5
0
−5
−10
28.0
28.1
28.2
(c)
Time (s)
JG01.23/11c

Fig. 11